

## Statistical Properties of Wiggler and Bending-Magnet Radiation from the Brookhaven Vacuum-Ultraviolet Electron Storage Ring

Malvin C. Teich

*Columbia Radiation Laboratory, Departments of Electrical Engineering and Applied Physics,  
Columbia University, New York, New York 10027*

Toshiya Tanabe and Thomas C. Marshall

*Department of Applied Physics, Columbia University, New York, New York 10027*

John Galayda<sup>(a)</sup>

*National Synchrotron Light Source, Brookhaven National Laboratory, Upton, New York 11973*  
(Received 17 September 1990)

The photoelectron counts of spontaneous light from the wiggler in the Brookhaven electron storage ring obey the negative-binomial distribution, in accord with the predictions of a multielectron, multimode theory. The bending-magnet light emerging from the Pyrex exit port of the storage ring obeys the Neyman type-A distribution.

PACS numbers: 42.55.Tb, 41.70.+t, 42.50.Bs

We have carried out a series of experiments on the photoelectron statistics associated with the radiation emitted from the vacuum-ultraviolet electron storage ring at the National Synchrotron Light Source at Brookhaven National Laboratory. The statistical properties of light emitted by electrons in a storage ring, and from free-electron lasers, are of interest inasmuch as sources such as these are being used in an increasingly broad range of applications.

There have been a number of theoretical investigations of the photon-number statistics of the radiation emitted from an electron beam as it propagates through a wiggler, i.e., the spontaneous emission from a free-electron laser.<sup>1-5</sup> A single electron gives rise to photons characterized by a Poisson photon-number distribution<sup>1</sup>  $P(n)$ , which has a variance given by

$$\text{Var}(n) = \langle n \rangle, \quad (1)$$

where  $\langle n \rangle$  is the photon-number mean. However, the radiation from an electron beam is more properly described by a multielectron theory. Several researchers<sup>2-5</sup> have shown that in this case

$$\text{Var}(n) = \langle n \rangle + \langle n \rangle^2 (1 - 1/N_e), \quad (2)$$

where  $\langle n \rangle = N_e \langle a \rangle$ , with  $N_e$  the (fixed) number of electrons in the bunch and  $\langle a \rangle$  the mean number of photons spontaneously emitted by a single electron during a pass through the wiggler. This formula can be viewed<sup>6</sup> as arising from a superposition of a fixed number  $N_e$  of independent, statistically identical coherent emissions, each of which contains a Poisson number of photons of mean  $\langle a \rangle$ . When  $N_e \gg 1$ , Eq. (2) reduces to the Bose-Einstein result associated with single-mode thermal light,<sup>6-8</sup> i.e.,

$$\text{Var}(n) = \langle n \rangle + \langle n \rangle^2. \quad (3)$$

Although Eqs. (2) and (3) are obtained using a multielectron theory, they are not directly applicable to the light observed from a radiating electron beam because the polarization properties of the light, and the finite photodetector counting time, area, and quantum efficiency must be taken into account. These factors require a multimode, rather than a single-mode, description of thermal light.<sup>9</sup> The detected photoelectrons are more properly described by the negative-binomial distribution,<sup>6,8-10</sup> which has a variance given by

$$\text{Var}(m) = \langle m \rangle + \langle m \rangle^2 / M. \quad (4)$$

Here  $\langle m \rangle = \eta \langle n \rangle$ , where  $\eta$  is the optical-system quantum efficiency, and  $M$  is the number-of-modes (degrees-of-freedom) parameter, to be described subsequently. The description provided in Eq. (4) is, indeed, applicable for describing the light from many types of lasers operated below threshold. For  $\eta = M = 1$ , we recover the Bose-Einstein result of Eq. (3).

In our experiments, a single pulse of electrons with an approximate duration of 480 psec at a point on the exit window moves around the ring once each 170.2 nsec. This group of electrons produces a pulse of light as it passes through a linear wiggler placed in the storage ring, and it also generates bending-magnet (synchrotron) radiation as it passes through each of the bending magnets in the ring. The light is always produced from the same group of electrons since the current decay time ( $\approx 100$  min) is much greater than the time of an experiment. The operating parameters of the wiggler and storage ring are provided in Table I.

The experimental arrangement for measuring the statistical properties of the wiggler light is schematically illustrated in Fig. 1. It makes use of an analog photoelectron-counting technique.<sup>11</sup> The radiation from the electrons as they pass through the wiggler takes the form

TABLE I. Wiggler (BNL designation U13-TOK) and storage-ring parameters used in our experiments. SQ represents the skew quadrupole parameter (SQ=300 and 0 correspond to tightly focused and loosely focused electron beams, respectively).

Wiggler period, $\lambda_0$	10 cm
Number of wiggler periods, $N$	22.5
Peak wiggler magnetic field, $B_0$	0.61 T
Wiggler strength parameter, $K$ ( $K = eB_0\lambda_0/2\pi\sqrt{2}mc^2$ )	4.0
Operating energy	$\approx 650$ MeV (wiggler light); $\approx 745$ MeV (bending-magnet light)
Operating current	$\approx 50$ mA (wiggler light); $\approx 150$ mA (bending-magnet light)
Horizontal damped emittance, $\epsilon_x$	$8.0 \times 10^{-8}$ m rad (SQ=300), $7.4 \times 10^{-8}$ m rad (SQ=0) (wiggler light); $1.5 \times 10^{-7}$ m rad (bending-magnet light)
Vertical damped emittance, $\epsilon_y$	$2.0 \times 10^{-8}$ m rad (SQ=300), $2.6 \times 10^{-8}$ m rad (SQ=0) (wiggler light); $> 2.8 \times 10^{-10}$ m rad (bending-magnet light)
Source size, $\sigma_h, \sigma_v$	1.0 mm, 0.32 mm (SQ=300), 0.96 mm, 0.36 mm (SQ=0) (wiggler light); 0.5 mm, $> 0.06$ mm (bending-magnet light)

of brief pulses of light with a center wavelength of 532 nm (at the fundamental) and a full width at half maximum (FWHM) of  $\approx 20$  nm. These light pulses pass through the Pyrex exit port of the ring and are directed through an optical interference filter with a center wavelength of 532 nm and a FWHM of 3.2 nm. The operating energy of the ring was adjusted so that the fundamental wavelength of the wiggler light would precisely match the maximum-transmission wavelength of the interference filter. The light was focused by a 50-mm-focal-length glass lens onto a Si *p-i-n* photodiode detector with a quantum efficiency of 0.78.

The photodiode output is passed through a pair of cascaded video amplifiers, each with an input impedance of 50  $\Omega$ , a voltage gain of 10, and a bandwidth of 500 MHz. These amplify the pulses by a factor of 100 and broaden their width from 480 psec to 5 nsec (see Fig. 1). The pulses are then fed into a gated-integrator-boxcar-averager module. This device high-pass filters the pulses to eliminate noise below 10 kHz, and provides an electronic gate with a 15-nsec width. It provides an output for every thousandth pulse, as selected by a cascade of three divide-by-ten counters which are triggered by the

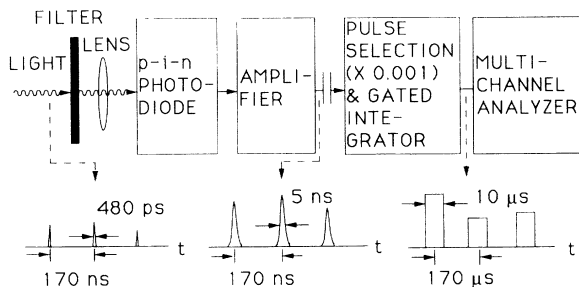


FIG. 1. Block diagram of the experimental arrangement used for the analog measurement of the photoelectron-counting distribution of wiggler light. The apparatus is operated in a slightly different configuration for obtaining the distribution of bending-magnet light (see text).

ring clock. The time between the selected pulses of light is therefore 170  $\mu$ sec, which is sufficiently slow for the electronics to register them. The selected pulses are then integrated and amplified (in this same processor) to produce a sequence of voltages, following each pulse, that is proportional to its integrated current, i.e., to its charge. A 10- $\mu$ sec-width sample of each of these voltages is obtained by using a digital-delay-pulse generator synchronized to the pulses, in conjunction with an integrated-circuit switch. This sequence of voltage samples, after suitable normalization, represents the numbers of photoelectrons per pulse. They are fed to a multichannel analyzer (2048 bins) which sorts them into a histogram that represents the photoelectron-counting distribution  $P(m)$ . The typical time to collect a distribution is  $\approx 5$  sec, during which a total of  $\approx 30000$  samples are collected (in some experiments only 15000 samples were registered).

The system noise was determined by feeding a sequence of identical deterministic electrical pulses (in place of the photodiode output) into the amplifier and then measuring the variance at the output of the multichannel analyzer as a function of the pulse level. The resultant noise-count variance was found to be approximately constant at  $\approx 3 \times 10^8$  for count means above  $5 \times 10^6$ ; however, it decreased with decreasing count mean below this value.

The experimental photoelectron-counting distribution  $P(m)$  is shown in Fig. 2(a) for the wiggler light. The mean photoelectron number for this particular distribution was adjusted to be  $\approx 9.8 \times 10^6$  by means of the neutral-density filter placed in front of the lens. The experimental distribution is nicely fitted by a negative-binomial theoretical distribution convolved with a zero-mean Gaussian distribution (with variance of  $3 \times 10^8$ ) representing the system noise. The experimentally determined number of modes is  $M \approx 54000$ .

In another set of experiments, the wiggler was effectively removed (by increasing the gap between the magnets) and the photoelectron-counting distribution of the

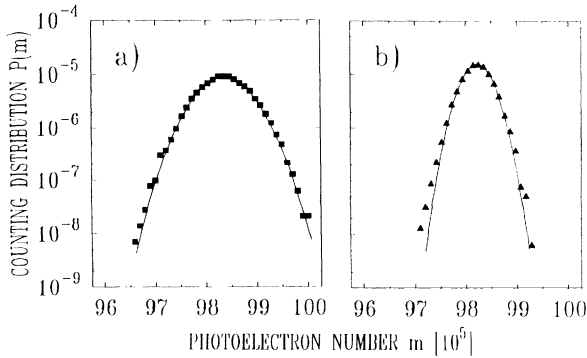


FIG. 2. (a) Squares represent the photoelectron-counting distribution  $P(m)$  vs the photoelectron number  $m$  for wiggler light from a tightly focused electron beam. The data are well fitted by a negative-binomial distribution convolved with a Gaussian representing the system noise (solid curve). (b) Triangles represent  $P(m)$  vs  $m$  for bending-magnet light. The data are well fitted by the Neyman type-A distribution convolved with the same Gaussian (solid curve).

bending-magnet light emerging from the Pyrex exit port of the storage ring was measured. The experimental arrangement is similar to that shown in Fig. 1 with the following exceptions (see Table I): The interference filter was removed to increase the photon flux entering the system; the operating energy of the ring was set at the normal value since it was not necessary to adjust the center wavelength of the light to the interference-filter maximum; the operating current was increased since the heating limitations imposed by the wiggler were not present; and the electron-beam emittance and source sizes were somewhat different.

The bending-magnet light in the ring is broadband with photon energies that stretch into the x-ray region. As a consequence of the short coherence time of this light, we would expect that the detected photons, if they were able to be measured directly, would obey the negative-binomial distribution with a value of  $M$  sufficiently large that the Poisson distribution would provide a good approximation.

The experimental photoelectron-counting distribution for the bending-magnet light is shown in Fig. 2(b). The mean photoelectron number was adjusted to be  $\approx 9.8 \times 10^6$ , the same as for the wiggler light shown in Fig. 2(a). The distribution associated with this light does not obey the Poisson distribution. Instead, it turns out to be well fitted by a Neyman type-A (NTA) distribution<sup>12-14</sup> convolved with the same zero-mean Gaussian noise distribution used for Fig. 2(a). The NTA distribution, which has a variance given by<sup>6,10,14</sup>

$$\text{Var}(m) = (1 + \eta\langle a \rangle)\langle m \rangle, \quad (5)$$

provides a good approximation for describing the statistics of luminescence light with an arbitrary spectrum.<sup>13,14</sup> Here  $\langle m \rangle = \eta\langle n \rangle$ , where  $\eta$  is the optical-sys-

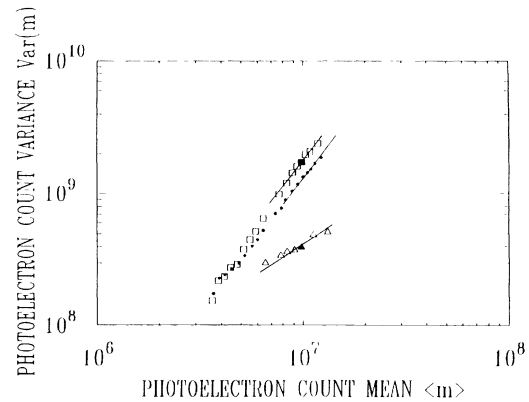


FIG. 3. Photoelectron-count variance vs count mean for wiggler light from a tightly focused electron beam (squares), a loosely focused electron beam (dots), and for bending-magnet light (triangles). The noise variance has been subtracted from the data as plotted. The count variance increases with the square of the mean for wiggler light, and directly in proportion to the mean for bending-magnet light. The solid square and triangle are the data points corresponding to the full counting distributions presented in Figs. 2(a) and 2(b), respectively.

tem quantum efficiency, and, in the context of luminescence,  $\langle n \rangle$  is the secondary photon-number mean and  $\langle a \rangle$  is the mean number of secondary photons per primary Poisson event.<sup>12</sup> It is determined from the data in Fig. 2 that  $\eta\langle a \rangle \approx 45$ .

We have experimentally verified that the wiggler light and bending-magnet light obey different functional forms for the variance, as given in Eqs. (4) and (5), respectively. The results are illustrated in Fig. 3 for wiggler light with a tightly focused electron beam (squares), a loosely focused electron beam (dots), and for bending-magnet light (triangles). The maximum photoelectron count mean ( $\approx 10^7$ ) was governed by the storage-ring current specified in Table I. Lower count means ( $\langle m \rangle$ ) were obtained by the use of the variable neutral-density filter in front of the lens and, to a lesser degree, by the loss of electrons during the duration of an experimental run. It is clear from Fig. 3 that the variance of the wiggler light does indeed vary as  $\langle m \rangle^2$ , as expected from Eq. (4) since  $\langle m \rangle \gg M$ , and the variance of the bending-magnet light varies as  $\langle m \rangle$  in accordance with Eq. (5).

Using Eq. (4), the number of modes  $M$  was determined from the experimental wiggler-light curves in Fig. 3 to be  $\approx 54000$  and  $78000$  for the tightly focused and loosely focused electron beams, respectively. It is difficult to precisely estimate the expected number of modes  $M$  without knowing the spatiotemporal correlation properties of the light. Nevertheless,  $M$  was estimated to be a product of three factors, associated with time, area, and polarization. We assumed that  $M \approx M_T M_A M_P \approx (T/\tau_c)(A/A_c)[2/(1+P)]$ , with  $T$  the counting time,

$\tau_c$  the coherence time of the light,  $A$  the photodiode active area,  $A_c$  the coherence area of the light, and  $P$  the degree of polarization. This expression is appropriate for cross spectrally pure light<sup>8</sup> when the first two factors are substantially greater than unity. These factors are roughly estimated to be  $M_T \approx 2450$ , using  $\tau_c \approx 0.2$  psec as determined by the Gaussian passband of the interference filter;  $M_A \approx 27.2$  and  $\approx 30.5$ , for the tightly focused and loosely focused beams, respectively (assuming that  $M_A$ , which depends on the emittance, can be reasonably represented as the calculated ratio of the total photon flux to the coherent photon flux<sup>15</sup>); and the measured degree of polarization  $P=0.87$ . The theoretically expected results for  $M$  are therefore  $\approx 71000$  and  $\approx 80000$  for the tightly focused and loosely focused electron beams, respectively, which are not in unreasonable agreement with the measured values given the large uncertainties involved. In other series of experiments, conducted using either longer pulse widths, unfocused wiggler light, or rectangular slits (in the horizontal or vertical direction), we obtained values of  $M$  that varied in the expected manner.

Using Eq. (5), it was determined that  $\eta\langle\alpha\rangle \approx 40$  for the collection of triangular data points in Fig. 3 [the specific data point used for Fig. 2(b) had a value  $\eta\langle\alpha\rangle \approx 45$ ]. One possible reason that the bending-magnet light emerging from the Pyrex exit port of the storage ring might obey the NTA distribution is as follows. A high-energy photon, when striking an optical material, can give rise to many visible photons through photoluminescence, as occurs in a scintillation crystal.<sup>13</sup> If the photon-number statistics of a pulse of synchrotron light inside the ring were Poisson, as expected, and the number of visible luminescence photons  $\alpha$  created per energetic synchrotron photon were also Poisson, the resulting photoelectron statistics would be describable by the NTA distribution.<sup>13</sup> The light emitted by a mechanism such as this would be diffuse, in accord with our observations. The photoluminescence explanation fails in one respect, however. From Eq. (5) it is seen that the quantum efficiency  $\eta$  multiplies the mean number of secondary photons per primary event  $\langle\alpha\rangle$ . The slope of the curve fitting the triangles in Fig. 3 should therefore vary as different neutral-density filters change the value of  $\eta$ , which it does not appear to do. The explanation of why the NTA distribution fits the bending-magnet light so well therefore requires further investigation.

With respect to the spontaneous wiggler light, we con-

clude that the applicability of the multimode thermal model is supported by the fit of the negative-binomial theoretical photoelectron-counting distribution to the data, by the observed quadratic dependence of the count variance on the count mean, and by the reasonable agreement of the theoretical estimates of the number of modes  $M$  with our observations. It is, perhaps, worthy of mention that the dependence of the variance on the mean was also quadratic for third-harmonic wiggler light at 532 nm, obtained by operating the ring at  $\approx 375$  MeV. It will be useful to conduct further studies to verify that other measures of the photoelectron point process<sup>6,8</sup> are consistent with the multimode thermal model for wiggler light.

We are grateful to C. Pellegrini for valuable discussions and suggestions. This work was supported by the Joint Services Electronics Program through the Columbia Radiation Laboratory, by Brookhaven National Laboratory, and by the Office of Naval Research.

(a)Present address: Argonne National Laboratory, Argonne, IL 60439.

<sup>1</sup>R. Bonifacio, *Opt. Commun.* **32**, 440 (1980).

<sup>2</sup>W. Becker and J. K. McIver, *Phys. Rev. A* **27**, 1030 (1983).

<sup>3</sup>W. Becker and J. K. McIver, *Phys. Rev. A* **28**, 1838 (1983).

<sup>4</sup>A. T. Georges, in *Free-Electron Generators of Coherent Radiation*, edited by C. A. Brau, S. F. Jacobs, and M. O. Scully [Proc. SPIE Int. Soc. Opt. Eng. **453**, 297 (1984)].

<sup>5</sup>J. Gea-Banacloche, *Phys. Rev. A* **31**, 1607 (1985).

<sup>6</sup>M. C. Teich and B. E. A. Saleh, in *Progress in Optics*, edited by E. Wolf (North-Holland, Amsterdam, 1988), Vol. 26, pp. 1-104, Eqs. (2.22), (2.23), and (2.56).

<sup>7</sup>S. Benson and J. M. J. Madey, *Nucl. Instrum. Methods Phys. Res., Sect. A* **237**, 55 (1985).

<sup>8</sup>B. Saleh, *Photoelectron Statistics* (Springer-Verlag, New York, 1978).

<sup>9</sup>G. Bédard, J. C. Chang, and L. Mandel, *Phys. Rev.* **160**, 1496 (1967).

<sup>10</sup>M. C. Teich and B. E. A. Saleh, *Opt. Lett.* **7**, 365 (1982).

<sup>11</sup>P.-L. Liu, L. E. Fencil, J.-S. Ko, I. P. Kaminow, T. P. Lee, and C. A. Burrus, *IEEE J. Quantum Electron.* **19**, 1348 (1983).

<sup>12</sup>M. C. Teich, *Appl. Opt.* **20**, 2457 (1981).

<sup>13</sup>B. E. A. Saleh, J. T. Tavolacci, and M. C. Teich, *IEEE J. Quantum Electron.* **17**, 2341 (1981).

<sup>14</sup>M. C. Teich and B. E. A. Saleh, *J. Mod. Opt.* **34**, 1169 (1987).

<sup>15</sup>K.-J. Kim, *Nucl. Instrum. Methods Phys. Res., Sect. A* **246**, 71 (1986).

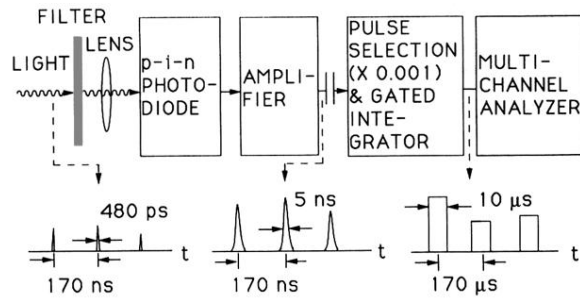


FIG. 1. Block diagram of the experimental arrangement used for the analog measurement of the photoelectron-counting distribution of wiggler light. The apparatus is operated in a slightly different configuration for obtaining the distribution of bending-magnet light (see text).